Characterization of inter-ELM magnetic oscillations on ASDEX Upgrade

F. Mink[1,2,*], E. Wolfrum[1], M. Maraschek[1], H. Zohm[1], L. Horváth[3], E. Viezzer[1], F.M. Laggner[4], M. Dunne[1], P. Manz[2,1], U. Stroth[1,2], the ASDEX Upgrade Team[1]

[1] *Max-Planck-Institut für Plasmaphysik, Boltzmannstr. 2, 85748 Garching, Germany*

[2] *Physik Department, E28, TUM, 85748 Garching, Germany*

[3] *York Plasma Institute, University of York, Heslington, York, YO105DD, UK*

[4] *Institute of Applied Physics, TU Wien, Fusion@ÖAW, 1040 Vienna, Austria*

Introduction

Edge localized modes (ELMs) occur as repetitive bursts of magnetohydrodynamic (MHD) activity in the high-confinement regime (H-mode) of tokamak fusion plasmas and might cause intolerably high heat fluxes onto the divertor target plates or the first wall in future fusion devices like ITER [1]. According to the broadly accepted peeling-ballooning (PB) model these MHD instabilities are driven by the steep edge pressure and current gradients, which are characteristic for the H-mode [2]. Nevertheless, the process that determines the onset of an ELM crash is not completely understood. It has been reported from different tokamaks that periodic MHD activities that might be connected to the ELM crash can be observed with defined toroidal mode numbers n between ELM bursts [3, 4].

Here the toroidal mode number n of inter-ELM phenomena on ASDEX Upgrade is investigated. Their development is connected to the development of the transport across the separatrix. Furthermore the poloidal mode number m is calculated to give an estimate for the radial position in terms of the safety factor $q = m/n$.

From linear PB stability analysis higher mode numbers of ELM associated modes are expected for higher collisionality ν^*. In order to investigate this effect mode numbers were determined for increasing ν^* in an experiment by increasing the density.

Characterization of inter-ELM phenomena

To resolve different phases during the ELM cycle an ASDEX Upgrade discharge (#28767) with a stationary phase from 2.0 to 2.5 s containing 25 ELMs with low ELM frequency of about $f_{\mathrm{ELM}} = 50\,\mathrm{Hz}$ was chosen. Other parameters are $I_{\mathrm{P}} = 0.8\,\mathrm{MA}$, $P_{\mathrm{Heat}} = P_{\mathrm{NBI}} + P_{\mathrm{ECRH}} = 2.5 + 1.5\,\mathrm{MW}$, $|B_{\mathrm{t}}| = 2.5\,\mathrm{T}$ and line integrated core electron density $n_{\mathrm{e}} = 6.0 \cdot 10^{19}\mathrm{m}^{-2}$.

Figure 1 shows an ELM synchronized spectrum from the outboard midplane magnetic pick-up coils measuring the radial magnetic field variation $\dot{B}_r$ together with the ELM synchronized divertor shunt current signal. As the divertor shunt current is essentially proportional to the temperature gradient at the divertor target plate it is a measure for the transport across the separatrix. A detailed description of the synchronization mechanism can be found in [5, 6].

*Corresponding author email: felician.mink@ipp.mpg.de, telephone: +49-89-32 99-1027

From the magnetic spectrum several phases can be identified in terms of their mode activity. The phases are the pre-ELM phase, the ELM-phase and four different post-ELM phases. In the first post-ELM phase there is almost no magnetic activity besides the one from a core mode ($f_c \leq 10\,\mathrm{kHz}$). The second, third and fourth phases undergo a transition at sharply defined times after the ELM onset from low ($\leq 50\,\mathrm{kHz}$) to medium (25–150 kHz) to high (200–250 kHz) frequency fluctuations. Phase IV can vary in length and therefore causes most of the scatter in the ELM frequency. In the pre-ELM phase both high and medium frequency fluctuations are visible and the ELM crash has a broad spectrum of frequencies where low frequencies are most dominant ($\leq 25\,\mathrm{kHz}$). All these phases align well with the transport behavior, visualized by the measured divertor shunt currents, Figure 1 (b). The transport is high during the ELM phase, while it decreases strongly when there is no magnetic activity in phase I. The transport increases again when the medium frequency fluctuation sets in and it equilibrates in phase IV. Besides the transport these phases also align with the pedestal parameters [5]. Both together show the connection of the mode activity to the pedestal development.The development of the frequency in the ELM cycle is caused by both, the development of mode numbers and the ExB velocity.

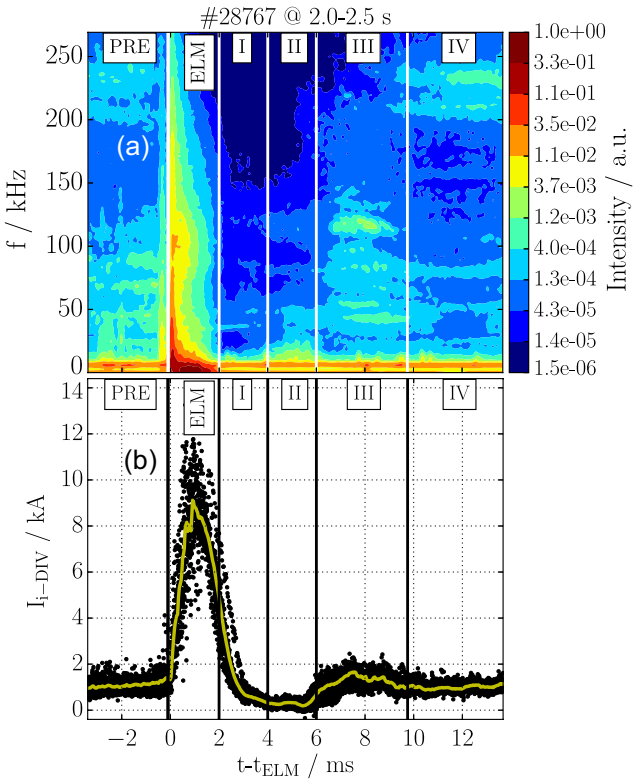

Figure 1: *(a) ELM synchronized spectrum with six distinct phases during the ELM cycle and (b) ELM synchronized data points of the inner divertor shunt current together with its smoothed signal.*

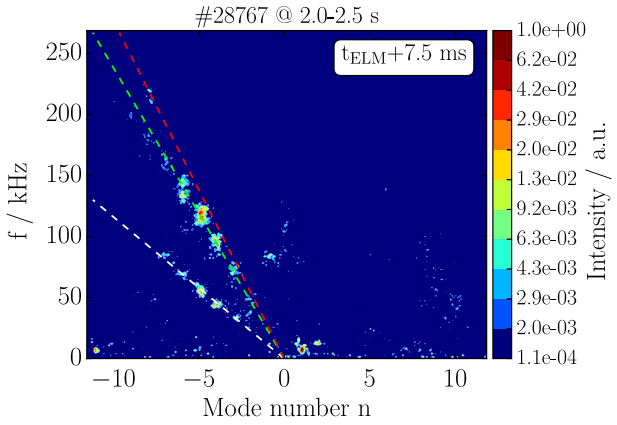

Figure 2: *ELM synchronized mode number histogram of the time windows around 7.5 ms after the ELMs. Red, green and white dashed lines indicate mode branches with different f/n values.*

Figure 2 shows the average mode number distribution for the different participating frequencies in phase III of the ELM cycle. From this mode number histogram it can be seen that several mode numbers are participating and that three so called branches (marked by the three dashed lines) exist in this phase. These branches are defined by the same f/n value. This means that single mode numbers forming these branches have all the same propagation velocity and

are therefore most probably located at the same radial position in the plasma. In this phase III the most dominant toroidal mode number is $n = -5$, where the negative sign means that this structure propagates in the electron diamagnetic drift direction. The $n = -5$ structure appears on the medium and the low velocity branch (green and white dashed lines). The high velocity branch (red dashed line) has only very weak activity with $n = -8$, $f = 220\,\mathrm{kHz}$ for this time frame but becomes dominant in phase IV and makes room again for low frequencies just before the ELM crash. The f/n value determines the velocity of the mode branches which can be compared to the ExB velocity close to the plasma edge in order to determine the position of the branches. Such a comparison shows that the mode branches appear close to the ExB minimum in the edge region but an exact position cannot be determined as the intrinsic velocities of the modes are unknown [6]. To further analyse the position of these different mode branches the

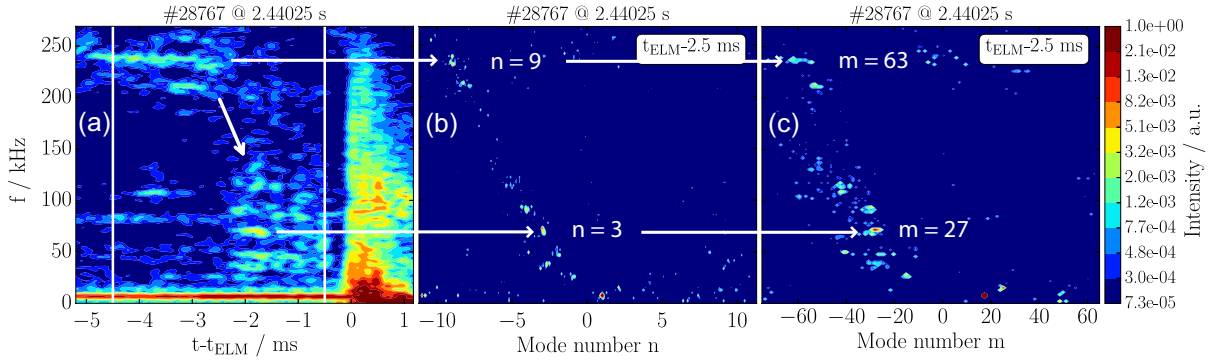

Figure 3: *(a) ELM synchronized spectrum and mode number histograms for the (b) toroidal and (c) poloidal mode number.*

time point just before one single ELM crash was chosen and analysed in terms of the appearing m and n mode numbers. Figure 3 (a) shows a spectrum relative to one single ELM crash. The time frame in which the mode numbers are evaluated is marked by white lines and a jump in frequency is marked by a white arrow. The mode number results are shown in (b) and (c), which share the frequency axes with (a). Again two different branches are visible. The first and faster one (similar to the red dashed line in Figure 2) has a dominant mode structure of $(m,n) = (63,9)$ where the second one (similar to the green dashed line in Figure 2) has a structure of $(27,3)$ which implicates different q positions, namely $q = 7$ and $q = 9$. The modes are therefore placed very close to the separatrix ($q_{95} = 5.5$), where the high frequency branch is slightly more inside than the low frequency branch. This also fits to the shape of the ExB velocity, which has its minimum at around $q = 7$ for this discharge and is zero at the separatrix.

In an effort to link these observations to the PB model a discharge is analyzed, in which ν^* is increased by increasing the fueling level. Figure 4 shows the three ELM synchronized spectra with the dominant toroidal mode numbers of inter-ELM edge modes for this discharge. The white arrows mark the high mode number fluctuations which are associated with modes placed in the ExB minimum. The red arrows mark the medium mode number fluctuations that are a result of modes placed slightly further outside. The result from a peeling-ballooning analysis

with MISHKA-fast shows that with increasing density the most unstable mode numbers increase from $n = 10$ to $n = 15$ and $n = 20$ [7]. The experimentally evaluated inter-ELM mode numbers do not follow this trend. They change only very slightly and even in the wrong direction, i.e. to lower n at higher ν^*. In agreement with previous observations, the high frequency branch decreases its frequency, which is due to the fact that it rotates with the velocity of the ExB minimum, which scales inversely with density [5], whereas the medium frequency branch changes only slightly as it is off the minimum.

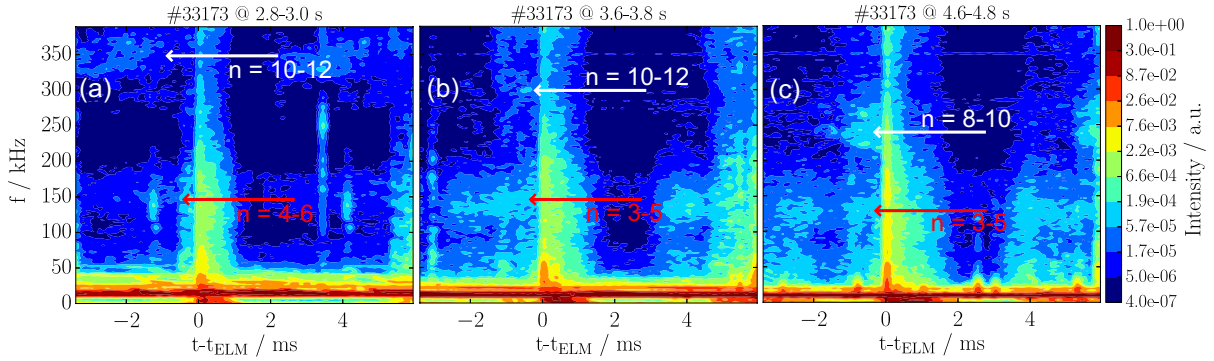

Figure 4: *ELM synchronized spectra for three time intervals with different fueling levels and therefore different ν^*: (a) low fueling, (b) medium fueling and (c) high fueling.*

In summary we can state the following. During the ELM cycle several mode branches exist with toroidal mode numbers in the range of $n = 1 - 10$ at different positions between the ExB minimum and the separatrix. Their rotation is caused by the ExB velocity and maybe an additional phase velocity. For each dominant mode branch different transport characteristics are observed and in the discharge shown here, a jump of intensity from the inside branch to the outside branch takes place a few ms before the ELM crash. For experiments with increasing ν^* the ideal PB stability analysis yields a strong increase in dominant n, whereas only slight changes (in the opposite direction) are observed for the modes prior to ELMs.

Acknowledgement

This work has been carried out within the framework of the EUROfusion Consortium and has received funding from the Euratom research and training programme 2014-2018 under grant agreement No 633053. The views and opinions expressed herein do not necessarily reflect those of the European Commission.

F. M. Laggner is a fellow of the Friedrich Schiedel Foundation for Energy Technology.

References

[1] A. Herrmann et al., Journal of Nuclear Materials, **313** (2003)
[2] H. Zohm, Plasma Physics and Controlled Fusion **38**, 2 (1996)
[3] C.P. Perez et al., Plasma Physics and Controlled Fusion **46**, 1 (2004)
[4] A. Diallo et al, Physics of Plasmas, **22**, 5 (2015)
[5] F.M. Laggner et al., Plasma Physics and Controlled Fusion, **58**, 6 (2016)
[6] F. Mink et al., Plasma Physics and Controlled Fusion, submitted 2016
[7] M. Dunne et al., Plasma Physics and Controlled Fusion, submitted 2016